

Out of Equilibrium Characteristics of a Forced Translocating Chain through a Nanopore

Aniket Bhattacharya^{1,*} and Kurt Binder²

¹*Department of Physics, University of Central Florida,*

Orlando, Florida 32816-2385, USA

²*Institut für Physik, Johannes Gutenberg-Universität Mainz,*

Staudinger Weg 7, 55099, Mainz, Germany

(Dated: February 7, 2020)

Abstract

Polymer translocation through a nano-pore in a thin membrane is studied using a coarse-grained bead-spring model and Langevin dynamics simulation with a particular emphasis to explore out of equilibrium characteristics of the translocating chain. We analyze the out of equilibrium chain conformations both at the *cis* and the *trans* side separately either as a function of the time during the translocation process or as a function of the monomer index m inside the pore. A detailed picture of translocation emerges by monitoring the center of mass of the translocating chain, longitudinal and transverse components of the gyration radii and the end to end vector. We observe that polymer configurations at the *cis* side are distinctly different from those at the *trans* side. During the translocation, and immediately afterwards, the chain is clearly out of equilibrium, as different parts of the chain are characterized by a series of effective Flory exponents. We further notice that immediately after the translocation the last set of beads that have just translocated take a relatively compact structure compared to the first set of beads that translocated earlier, and the chain immediately after translocation is described by an effective Flory exponent 0.45 ± 0.01 . The analysis of these results is further strengthened by looking at the conformations of chain segments of equal length as they cross from the *cis* to the *trans* side, We discuss implications of these results to the theoretical estimates and numerical simulation studies of the translocation exponent reported by various groups.

PACS numbers: 87.15A-,87.15.H-, 36.20.-r

*Author to whom the correspondence should be addressed; Electronic address: aniket@physics.ucf.edu

I. INTRODUCTION

Despite a large number of theoretical and numerical studies voltage driven polymer translocation through a nanopore[1, 2] and its prospective applications has remained an active field of research with many open questions. Initial theoretical work of Chuang Kantor and Kardar[3], Kantor and Kardar[4], Sung and Park[5], Muthukumar[6], followed by more recent theoretical studies by Dubbledam *et al.*[7, 8], Panja *et al.*[10, 11, 12], Sakaue[13], and Slater *et al.* [14] has sparked renewed interests and numerical work[15]-[28]. In a recent paper[28] for the case of forced translocation we have compared predictions from theoretical studies with those obtained using Langevin dynamics simulation results. We observed that the driven translocation process is dominated by out of equilibrium characteristics which may lead to misinterpretation of the time averaged data for the translocated chain. We further noticed that one needs to look at the chain segments at the *cis* and the *trans* side separately to get a true picture of the translocation process.

The purpose of this paper to study the aforementioned out of equilibrium characteristics of relevant physical parameters in detail by monitoring the *trans* and the *cis* characteristics separately as a function of the chain segment $N - m(m)$ at the *cis(trans)* compartments. To emphasize the role of out of equilibrium aspects we have taken a *reductio ad absurdum* approach. We first hypothesize that the chain undergoing forced translocation is at each instant of time in equilibrium; we then demonstrate violation of this hypothesis for the forced translocation process in several physical quantities obtained from simulation studies. Of course, we also have carried out simulation studies for the unbiased translocation so that these results can serve as reference for the specific pore-wall geometry that we choose. In the next section we describe the model. In section III we present the results from Langevin dynamics simulation. In section IV we discuss in detail the relevance of these results

II. THE MODEL

We have used the “Kremer-Grest” bead spring model to mimic a strand of DNA [29]. Excluded volume interaction between monomers is modeled by a short range repulsive LJ

potential

$$\begin{aligned}
 U_{LJ}(r) &= 4\epsilon\left[\left(\frac{\sigma}{r}\right)^{12} - \left(\frac{\sigma}{r}\right)^6\right] + \epsilon \text{ for } r \leq 2^{1/6}\sigma \\
 &= 0 \text{ for } r > 2^{1/6}\sigma .
 \end{aligned}$$

Here, σ is the effective diameter of a monomer, and ϵ is the strength of the potential. The connectivity between neighboring monomers is modeled as a Finite Extension Nonlinear Elastic (FENE) spring with

$$U_{FENE}(r) = -\frac{1}{2}kR_0^2 \ln(1 - r^2/R_0^2) ,$$

where r is the distance between consecutive monomers, k is the spring constant and R_0 is the maximum allowed separation between connected monomers. We use the Langevin dynamics with the equation of motion

$$\ddot{\vec{r}}_i = -\vec{\nabla}U_i - \Gamma\dot{\vec{r}}_i + \vec{W}_i(t) .$$

Here Γ is the monomer friction coefficient and $\vec{W}_i(t)$, is a Gaussian white noise with zero mean at a temperature T , and satisfies the fluctuation-dissipation relation:

$$\langle \vec{W}_i(t) \cdot \vec{W}_j(t') \rangle = 6k_B T \Gamma \delta_{ij} \delta(t - t') .$$

The purely repulsive wall consists of one monolayer of immobile LJ particles of diameter 1.5σ on a *triangular lattice* at the xy plane at $z = 0$. The pore is created by removing the particle at the center. Inside the pore, the polymer beads experience a constant force F and a repulsive potential from the inside wall of the pore. The reduced units of length, time and temperature are chosen to be σ , $\sigma\sqrt{\frac{m}{\epsilon}}$, and ϵ/k_B respectively. For the spring potential we have chosen $k = 30$ and $R_{ij} = 1.5\sigma$, the friction coefficient $\Gamma = 1.0$, and the temperature is kept at $1.5/k_B$ throughout the simulation.

For the case of unbiased translocation we have chosen chain lengths $N = 17, 33, 65, 129, \text{ and } 257$ and put the middle monomer symmetrically inside the pore ($z = 0$) with equal number of monomers at the *cis* and the *trans* side and let the translocation occur either toward right or left. We have checked that for a large number of repeated trials the probability for translocation from right to left or vice versa is the same. In this case each chain is equilibrated keeping the middle monomer at the fixed location $z = 0$ inside the pore and then releasing it for translocation. The results are averaged over at least for 2000 trials.

For the case of forced translocation we carried out simulations for chain lengths N from 8 – 256 for several choices of the biasing force $F = 2, 4, 6,$ and 12 respectively. For most cases we show the results for $F = 6$. Initially the first monomer of the chain is placed at the entry of the pore. Keeping the first monomer in its original position the rest of the chain is then equilibrated for times at least an amount proportional to the $N^{1+2\nu}$. The chain is then allowed to move through the pore driven by the field present inside the pore. When the last monomer exits the pore we stop the simulation and note the translocation time and then repeat the same for 5000 such trials. In comparison to reality, our model is drastically simplified: we deal with a neutral homopolymer without explicit solvent, there are neither hydrodynamic interactions nor long range electrostatic forces. However, our model is of the same type as most of the currently available theoretical work. We feel that this simple limiting case needs to be understood first, before more realistic cases may be tackled.

III. RESULTS

As mentioned in the introduction that along with the results for the forced translocation we also present results for the unbiased case, as necessary for comparison. Except for Fig. 4 where plots are shown for four different biases the remaining figures for the forced translocation refer to $F=6.0$. We have monitored the mean first passage time (MFPT), the transverse and longitudinal components of the gyration radii at the *cis* and the *trans* side, the end-to-end vector, and the center of masses of the segments residing at the *cis* and the *trans* sides. In each case for a quantity A the notation $\langle A \rangle$ refers to the average over 2000-5000 independent runs.

A. Translocation exponent for the unbiased translocation

First, as a reference we have checked the scaling exponents for the unbiased translocation for the choice of parameters used here. This is shown in Fig. 1 where we find $\langle \tau \rangle \sim N^{2.2}$ and $\langle R_g \rangle \sim N^{0.61}$. Therefore we verify that for unbiased translocation the translocation exponent α ($\langle \tau \rangle \sim N^\alpha$) scales as $\langle \tau \rangle \sim N^{1+2\nu}$ as previously found by us[15] in a slightly different context using Monte Carlo (MC) and others in 2D[16, 27].

B. Mean first passage time (MFPT)

Fig. 2 shows the MFPT time for a forced translocating chain as a function of the translocated segment m for several chain lengths. We include this curve for future discussions as one readily gets the average translocation time $\langle \tau(m) \rangle$ of a particular monomer index m or vice versa. For larger chain lengths the non-linear nature in the form of an S shaped curve becomes more prominent where we notice that the curvature is negative (concave) for $m < N/2$ and becomes positive for $m > N/2$. The last few beads take relatively much shorter time to translocate.

C. What is the coordinate of $Z_{CM}(N/2)$?

If the translocating chain were in local equilibrium then one would expect that when the chain is half way through the translocation process the position of the z component of the center of mass $Z_{CM}(N/2)$ should be located symmetrically with respect to the *cis* and the *trans* side. This should correspond to $z = 0$ for our choice of coordinate system. Fig. 3 shows the distribution of the location of $Z_{CM}(N/2)$ and the average value $\langle Z_{CM}(N/2) \rangle$ for three different chain lengths. We note that with increasing chain length the location of $Z_{CM}(N/2)$ goes deeper in the *cis* side of the chain. When we plot $\langle Z_{CM}(N/2) \rangle$ as a function of the chain length N shown in Fig. 4 we note that after a certain *crossover length* the distance increases approximately linearly with the chain length for larger chains. It is also interesting to observe that this crossover length increases as the bias becomes small. This implies that finite chain lengths effects become progressively smaller as a function of the increasing bias, a result that seems counter-intuitive.

D. Behavior of $Z_{CM}^{cis}(m)$ and $Z_{CM}^{trans}(m)$

This asymmetry in the location of $\langle Z_{CM}(N/2) \rangle$ becomes more obvious when we look at the positions of the center of masses on the *cis* side ($Z_{CM}^{cis}(m)$) and the *trans* side ($Z_{CM}^{trans}(m)$) separately. Again, if the local equilibrium condition should hold, one would expect that as a function of the *trans* and *cis* segments the behavior of $Z_{CM}^{trans}(m)$ and $Z_{CM}^{cis}(m)$ should be the same. For comparison, and as a reference we first show the plot for the case of unbiased translocation in Fig. 5 where we notice that the longitudinal and the transverse components

of the gyration radii for both the *cis* and *trans* segments are almost indistinguishable as anticipated. We further note that for large portion of the chain except for very small and large values of the monomer index $\langle Z_{CM}^{cis,trans} \rangle \sim m^{0.56}$. If the configurations of the chains in the case of unbiased translocation just realize a sequence of equilibrium configurations, we expect $\langle Z_{CM}^{cis,trans} \rangle \sim m^\nu$ with $\nu \approx 0.59$ the equilibrium Flory exponent, when $m \rightarrow \infty$. Although the effective exponent (0.56) is somewhat smaller, it is clear that in this case the translocating chains are close to equilibrium. This should be contrasted with the corresponding case for the forced translocation where we observe a very different behavior as shown in Fig. 6 for the *cis* and the *trans* segments. Using Fig. 2 one can translate the figure from the variable m to the corresponding MFPT. One notices that the *cis* component increases almost linearly for $0 < m < N/2$ and scales as $\langle Z_{CM}^{cis}(m) \rangle \sim m^{0.91}$, whereas the *trans* part after a linear rise for small m , increases at a much slower rate compared to the *cis* part. We further notice $\langle Z_{CM}^{trans}(m) \rangle \sim m^{0.45}$, the value of the slope (0.45) in this case exactly half of the corresponding value of the *cis* part. We notice similar qualitative behavior for $\langle R_g^{cis}(m) \rangle$ and $\langle R_g^{trans}(m) \rangle$ and defer the physical explanation of this behavior to subsection-F.

E. Gyration radii: time dependence

To get a better idea of the out of equilibrium characteristics of the forced translocating chain we have compared the time dependence of gyration radii with those for the unbiased chain shown in Fig. 7. For unbiased translocation $\langle R_{gl} \rangle > \langle R_{gt} \rangle$ is due to the presence of the wall that breaks the isotropy symmetry and gyration radius along the translocation direction becomes larger when calculated for the entire chain. This anisotropy occurs already for a polymer chain anchoring with a chain end at a flat impenetrable surface (a “polymer mushroom”). For unbiased translocation, the typical chain conformations are those of equilibrium mushrooms containing m and $N - m$ segments, respectively. When we compare these time dependencies with those for the chain undergoing forced translocation we notice that the forced chain undergoes considerable variation in its size. However, despite this large variation in size when we calculate the average gyration radii we find $\langle R_g \rangle \sim N^\nu$ [28]. Therefore, if one does not plot and see this explicit time dependence, one would tend to make an assumption that only one bead of the chain is driven inside the pore, and there-

fore the chain is still described by the equilibrium Flory exponent[4]. The argument that immediately comes to ones mind that the variations are cancelled (Fig. 7(b)) which we find is wrong and it is inappropriate to describe the chain by a single exponent. In the next subsection we will provide the correct physical reason why the chain is still described the equilibrium Flory exponent.

F. Gyration radii components at the *cis* and *trans* side

To further demonstrate the out of equilibrium aspects of the driven translocating chain we have monitored time dependence of the transverse and longitudinal components of the *cis* and *trans* part of the gyration radii separately and compared these characteristics with those for the unbiased translocation. Fig. 8 shows the plots of the transverse and longitudinal components for the *cis* side ($\langle R_{gt}^{cis}(m) \rangle$, $\langle R_{gl}^{cis}(m) \rangle$) and for the *trans* side ($\langle R_{gt}^{trans}(m) \rangle$, $\langle R_{gl}^{trans}(m) \rangle$) separately for the unbiased translocation. As expected, except for the few first and last beads (which may depend on the local condition) the conformations for the *cis* and *trans* parts are the same[30]. We further notice that for small values of segments m $R_{gl} > R_{gt}$; however this difference might arise due to finite chain length that vanishes for large values of m . Within our error limits, these data are compatible with a scaling of all these radii according to a law $R \propto N^\nu$ with $\nu \approx 0.59$ being the expected Flory exponent.

For the case of forced translocation (Fig. 9) one immediately notices that the $\langle R_g(m) \rangle$ of the chain on the *cis* and *trans* side are described by different effective Flory exponents. The effect is most pronounced for the longitudinal component. We have calculated the slopes for $N/8 < m < N/4$ and find that $\langle R_{gl}^{trans}(m) \rangle \sim m^{0.6}$ and $\langle R_{gl}^{cis}(m) \rangle \sim m^{0.8}$. This result is consistent with the recent theory proposed by Sakaue[13] based on the propagation of tension along the chain. During the forced translocation process at early time ($m \ll N$) the translocated monomers relax faster and are described roughly by the equilibrium Flory exponent. However, during the short time needed that a small number of m monomers are pulled through the pore by the force, the remaining $N - m$ segments do not have enough time to equilibrate their configuration. One can think of this effect as the size of $R_g^{cis}(N - m)$ remaining the *sameas* $R_g^{cis}(N)$ but with a few *less* number of monomers because of those that have translocated. This makes the effective Flory exponent higher on the *cis* side at the early stage of the translocation process. As time proceeds the number

of monomers on the *cis* side also decreases causing the slope (Fig. 9) also to decrease). This difference in behavior of $R_g^{trans}(m)$ and $R_g^{cis}(m)$ as manifested in our simulation studies should serve as useful information for the development of detailed analytical theories of forced polymer translocation through a nano pore. Since the translocation time in the case of forced translocation for large N is much smaller than the Rouse time needed to equilibrate a chain, the conformations of the chains that just have translocated are much too compact (Fig. 10), leading to a scaling $R_g^{trans} \sim N^{\nu_{eff}}$ with $\nu_{eff} \sim 0.5$.

G. Analysis of the subchain relaxation on *cis* and *trans* sides

In order to get a better picture of the chain relaxation at the *trans* and *cis* side we have further investigated the relaxation of sub-chain conformations during the translocation process. Since this analysis requires a relatively longer chain we will restrict our discussion for a chain of length $N = 256$ consisting of either 8 or 16 subchains each of length 32 or 16. For the rest of the discussion in this section let's consider 8 subchains each consisting of 32 monomers (the qualitative features for the subchains of length 16 are very similar). Let's denote these subchains of length 32 as n_i ($i = 1, 2, \dots, 8$). Therefore the i -th chain segment n_i consists of monomers having indices from $(i-1)*32+1$ to $i*32$. At the start of the translocation process initially, all subchains are in equilibrium, and have their values for their end-to-end distance and gyration radius components as appropriate for a calculation done for the mushroom in equilibrium, which is not yet translocating and the entire chain being located at the *cis* side. Once the translocation starts, we study all these subchains at times when the last monomer of each segment n_i has just translocated from the *cis* to the *trans* side. Therefore, for the chain length $N=256$ consisting of 8 subchains, at the end of a successful translocation process we will have 8 different subchain conformations starting with $n_{trans} = 1$ and $n_{cis} = 7$ until all the segments are translocated when $n_{trans} = 8$ and $n_{cis} = 0$. We then analyze these subchain conformations averaged over 2000 repeated trials.

It is expected that the subchain n_i which has just translocated and its two neighboring subchains n_{i-1} and n_{i+1} will be affected by the driving force and out of equilibrium characteristics will dominate most. But the chain segments which are further away will progressively be closer to equilibrium. In other words, by the time the subchain n_i has just translocated, the translocated chain segments $n_1, n_2, n_3 \dots n_{i-2}$ will have more time to relax

(as a function of the decreasing segment index i) compared to the segment n_{i-1} , while the segments $n_8, n_7 \dots$ will remain mostly in equilibrium and hardly feel that the subchain n_i has just translocated. Thus if we look at the conformations for all the segments at these times we expect to see that the *cis*-subchain closest to the pore is mostly stretched with a higher value of the Flory exponent, while the *trans*-subchain which just finished translocation is compressed most with a lower value of the Flory exponent. These higher(lower) value at the *cis(trans)* side will progressively taper towards the equilibrium value on either side of the pore. The increased value of the Flory exponent will appear like a propagating defect.

In the accompanying Fig. 12(subchain length 16) we have plotted the gyration radii and the corresponding transverse and the longitudinal components for the chain segments at times immediately after subchains 1, 3, \dots 15 have translocated. The corresponding scenario for the analysis using subchain length 32 is shown Fig. 13. In Figs. 12 and 13 we kept the vertical scale the same for all the graphs for ready comparison of the gyration radii at different stage of the translocation process. First, one notices that after the translocation process, the chain is still compressed. Secondly, at the *trans* side the slope of the line connecting the points increases monotonically (not shown) from the left to the right, the gyration radii of the *trans*-segment closest to the pore being the least (such as in Fig. 13(f) and Fig. 13(g)). This is due the fact, as stated above, that the farthest *trans*-segment have more time to approach equilibrium configuration from its initial compressed state at the entry of *trans* side. Likewise, on the *cis* the slope of the curve joining the *cis* segments decreased monotonically for the same reason that the farthest segment is still in equilibrium and the *cis*-segment closest to the pore is mostly stretched. It is clear from the data that subchain relaxation proceeds exactly the way as contemplated in above.

H. Properties of a translocated chain

In order to interpret the properties of a chain which has just translocated, we introduce the concept of a time-dependent correlation length $\xi(t)$ describing the range over which (on the *trans* side of the membrane) excluded volume effects are established (at a time t after the translocation process has begun). We start from the fact that for the Rouse model with excluded volume interactions the length (chain radius R) and relaxation time τ are related as $\tau \propto R^z \propto N^{\nu z} = N^{2\nu+1}$ where the dynamic exponent $z = 2 + 1/\nu$. Consider now

the ‘‘Gedankenexperiment’’ that for a Gaussian chain at time $t = 0$ the excluded volume interactions are suddenly switched on. Then the chain starts to swell, its radius will grow from the Gaussian size ($R \propto N^{1/2}$) to the swollen size ($R \propto N^\nu$ with $\nu \approx 0.59$) during the time τ . At time t , one can envisage this gradual swelling that on a length scale $\xi(t)$ excluded volume has already been established, but not on scales much larger than $\xi(t)$; so the chain is a Gaussian string of blobs of size $\xi(t)$. One expects that $\xi(t) \propto t^{1/2}$ and then indeed there is a smooth crossover to the equilibrium size $R \propto N^\nu$ at $t = \tau$, $\xi(\tau) \propto N^\nu$.

In a forced translocation process, the monomers move to the *trans* side so fast that the equilibrium structure cannot develop on the scale of the full chain, but only the first N_{eq} monomers that have passed the pore can develop in their configuration the proper correlations due to excluded volume. We can estimate (for large enough F) this number N_{eq} by

$$\begin{aligned} \xi(\tau) &\sim N_{eq}^\nu, \quad \tau \sim N^\alpha/F, \quad \xi(\tau) \propto \tau^{1/z} \Rightarrow N_{eq} \\ &\sim \xi(\tau)^{1/\nu} \propto \tau^{1/(\nu z)} \propto N^{\alpha/\nu z} F^{-1/\nu z} = N^{\alpha/(2\nu+1)} F^{-1/(2\nu+1)} \end{aligned} \quad (1)$$

For the measured value of α the corresponding size is

$$R = \xi(\tau) \propto N^{\alpha\nu/(2\nu+1)} F^{-1/(2\nu+1)} \quad (2)$$

For $\alpha = 1.36$ [28] we obtain $\alpha\nu/(2\nu + 1) = 0.37$ while the value for α proposed in [4], $\alpha = 1 + \nu$ would yield $\alpha\nu/(2\nu + 1) = 0.43$. Of course, the estimate in Eq. 2, based on the N_{eq} monomers that had enough time to equilibrate during the translocation time, is only a lower bound for the actual radius R_{trans} of the translocated chain, because the additional $N - N_{eq}$ monomers (translocated, but not yet equilibrated) can lead to some further increase in an uncorrelated way (so $R \propto N^{1/2}$ probably is an upper bound). However, it remains a challenge to clarify whether the effective exponent $\nu_{eff} \approx 0.45$ observed for several properties on the *trans* side (Fig. 6, Fig. 10) really describes the asymptotic regime or is still affected by some correction to scaling effects; recall that in the data for unbiased translocation effective exponents vary from $\nu_{eff} \approx 0.55$ (Fig. 5) to $\nu_{eff} \approx 0.63$ (fig. 1) around the true asymptotic value $\nu \approx 0.59$.

Another problem that is not understood is to explain the rather different behavior of R_{gl} and R_{gt} for large values of m (close to N) in Fig. 14. These data are presumably dominated

by the $N - N_{eq}$ monomers of the translocated chain that are still far from equilibrium. Therefore it is clear that the evolution of the translocated chain configuration with time (or with m , respectively) cannot be described in a simple manner.

Finally, it would be interesting to clarify the crossover between forced and unbiased translocation as $F \rightarrow 0$. Note that Eqs. 1, 2 do not apply in this limit. Rather a simple scaling assumption could be

$$\langle \tau \rangle = N^{2\nu+1} f(FN^{2\nu+1-\alpha}) \quad (3)$$

where the scaling function $f(\zeta)$ behaves as $f(0) = const$ (unbiased translocation) while $f(\zeta \gg 1) \propto 1/\zeta$ in order to recover Eq. 1 in the limit of large enough F . Fig. 4 is a first indication that in the structure of the chain there is indeed an interesting and nontrivial dependence on F , but clearly more work is needed to fully clarify the aspects of this behavior by extensive simulations, which are very time-consuming and therefore beyond the scope of the present work.

But a safe general conclusion is that the theory of forced translocation needs to adequately account for the non-equilibrium aspects of the translocation process and the resulting strong asymmetry of the properties of the *cis* and *trans* parts of the chain.

I. Distribution of the end to end length

To get a better idea of the out of equilibrium aspects of the translocating chain we have looked at the distribution of the transverse and longitudinal components of the end to end vector \mathbf{R} for the chain which has just translocated shown in Fig. 15. For comparison we have also shown the corresponding distribution of the equilibrated chain configurations located at the *cis* side at time $t = 0$ at the beginning of each translocation process. One immediately notices that the the distribution of \mathbf{R} is much more restricted compared to its equilibrium configuration.

IV. SUMMARY AND DISCUSSION

In summary, several aspects of forced polymer translocation are studied in this paper which explicitly point towards the out of equilibrium aspects of the translocation process.

In several cases we also furnish data for the unbiased translocation for identical parameters of the simulation. From the series of data one could say that immediately after the translocation starts till it ends, the entire chain is always out of equilibrium. However, the nature and extent of this out of equilibrium aspect is different at the *cis* and *trans* sides and evolves with time. The “subchain” analysis vividly demonstrates this aspect in terms of subchain linear dimensions, with which we may associate the effective Flory exponent which is clearly largest in the immediate vicinity of the *cis* side of the pore, and acquires a smaller value in the immediate vicinity of the *trans* side of the pore. Immediately after the translocation process clearly the entire chain is compressed and described by a lower value of the effective Flory exponent. On the contrary the *cis*-segments are described by a progressively higher value of the effective Flory exponent. In short, the bias at the pore makes the chain expanded and compressed at the *cis* and *trans* sides respectively, the chain tension being a function of the location of the segment (bead) with respect to the pore. This aspect was emphasized by Sakaue in a slightly different context. From the chain segment analysis we find that the translocation process can be viewed as a propagation of a “defect” in the value of the effective Flory exponent space in the opposite direction of translocation. Therefore, the analytic treatments in terms of one “slow” variable (s coordinate) is not adequate. Since the relaxation is different on the *cis* and *trans* side, one needs to incorporate additional slow variables to account for this *trans* – *cis* asymmetry[31].

With the propagating defect picture in mind let us now look at the possible scenario in the limit of very large chain. The defect will decay to its equilibrium value as shown in Fig. 16. How does the magnitude of the force dictate the correlation length of the decay of this defect ? Furthermore, we know that in the limit of force $\rightarrow 0$ the segment analysis will remain valid and the defect will go to zero as there will be no distinction between the *trans* and *cis* side. Can one recover Kantor-Kardar result from a finite size chain simulation with proper extrapolation ? While further work is needed to settle these issues we have initiated some work along this line in section-H. We hope that the qualitative description of polymer translocation in terms of a “defect” in the value of the effective Flory exponent will motivate further theoretical work to construct a more complete theory of forced translocation.

V. ACKNOWLEDGEMENT

A. B. appreciates the local hospitality at the Institut für Physik, Johannes-Gutenberg Universität, Mainz, where most of this work was done, and gratefully acknowledges the travel support from the Deutsche Forschungsgemeinschaft, SFB 625/A3 and from the Schwerpunkt für Rechnergestützte Forschung in den Naturwissenschaften (SRFN).

REFERENCES

- [1] J. J. Kasianowitch, E. Brandin, D. Branton, and D. Deamer, Proc. Natl. Acad. Sci. U.S.A. **93**, 13770 (1996); A. Meller, L. Nivon, E. Brandin, J. Golovchenko, and D. Branton, *ibid* **97**, 1097 (2000);
- [2] J. L. Li, M. Gershow, D. Stein, E. Brandin, and J. A. Golovchenko, Nat. Mater. **2**, 611 (2003); A. J. Storm, J. H. Chen, X. S. Ling, H. W. Zandbergen, and C. Dekker, *ibid* **2**, 537 (2003).
- [3] J. Chuang, Y. Kantor, and M. Kardar, Phys. Rev. E, **65**, 011802 (2001).
- [4] Y. Kantor and M. Kardar, Phys. Rev. E, **69**, 021806 (2004).
- [5] W. Sung and P. J. Park, Phys. Rev. Lett. **77**, 783 (1996)
- [6] M. Muthukumar, J. Chem. Phys. **111**, 10371 (1999).
- [7] J. L. A. Dubbledam, A. Milchev, V. G. Rostiashvili, and T. Vilgis, Phys. Rev. E **76**, 010801(R) (2007)
- [8] J. L. A. Dubbledam, A. Milchev, V. G. Rostiashvili, and T. Vilgis, Europhysics Letters **79** 18002 (2007).
- [9] J L A Dubbledam, A. Milchev, V. Rostiashvili, and T A Vilgis, J. Phys.:Condens. Matter **21** 098001 (2009).
- [10] J. K. Wolterink, G. T. Barkema, and D. Panja, *Phys. Rev. Lett.* **96**, 208301 (2006).
- [11] D. Panja, G. T. Barkema, and R. C. Ball, *J. Phys.: Condens. Matter* **19**, 432202 (2007); *ibid***20**, 075101 (2008).
- [12] H. Vocks, D. Panja, G. T. Barkema, and R. C. Ball, *J. Phys.: Condens. Matter***20**, 095224 (2008).

- [13] T. Sakaue, Phys. Rev. E **76** 021803 (2007).
- [14] M. G. Gauthier and G. W. Slater, J. Chem. Phys. **128** 065103 (2008); *ibid* **128** 205103 (2008).
- [15] A. Milchev, K. Binder, and A. Bhattacharya, J. Chem. Phys. **121**, 6042 (2004).
- [16] K. Luo, T. Ala-Nissila, and S-C. Ying, J. Chem. Phys. **124**, 034714 (2006).
- [17] K. Luo, T. Ala-Nissila, and S-C. Ying, J. Chem. Phys. **124**, 114704 (2006).
- [18] I. Huopaniemi, K. Luo, T. Ala-Nissila, S-C. Ying, J. Chem. Phys. **125**, 124901 (2006).
- [19] D. Wei, W. Yang, X. Jin, and Q. Liao, J. Chem. Phys. **126**, 204901 (2007)
- [20] K. Luo, T. Ala-Nissila, and S-C. Ying, and Aniket Bhattacharya J. Chem. Phys. **126** 145101 (2006); Phys. Rev. Lett. **99** 148102 (2007); *ibid* **100** 058101 (2008).
- [21] S. Matysiak, A. Montesi, M. Pasquali, A. . Kolomeisky, C. Clementi, Phys. Rev. Lett. **96** 118103 (2006).
- [22] S. Guillouzie and G. W. Slater, Physics Letters A **359**, 261 (2006).
- [23] M. G. Gauthier and G. W. Slater, Eur. Phys. J. E **25**, 17 (2008).
- [24] M. G. Gauthier and G. W. Slater, Phys. Rev. E **79**, 021803 (2009).
- [25] K. Luo, S. Ollila, I. Huopaniemi, T. Ala-Nissila, P. Pomorski, M. Karttunen, S-C. Ying, and A. Bhattacharya, Phys. Rev. E. **78** 050901(R) (2008).
- [26] V. V. Lehtola, R. P. Linna, and K. Kaski, Europhys. Lett. **85** 58006 (2009); Phys. Rev. E **78** 061803 (2008).
- [27] D. Wei and W. Yang, J. Chem. Phys. **126** 204901 (2006).
- [28] Aniket Bhattacharya, William H. Morrison, Kaifu Luo, Tapio Ala-Nissila, See-Chen Ying, Andrey Milchev, and Kurt Binder (to appear in Euro. Phys. J. E, 2009).
- [29] G. S. Grest & K. Kremer, Phys. Rev. A *33*, 3628 (1986);
- [30] For the case of unbiased translocation the *cis/trans* components are defined if the chain translocates from left(*cis*) to right(*trans*) or vice versa unlike the case of forced translocation where the applied bias uniquely defines the *cis* and the *trans* components.
- [31] AB gratefully acknowledges the conversation with Prof. W. Sung on this particular aspect of the translocation problem.

FIGURE CAPTIONS

Fig. 1: Scaling plot (log-log scale) of the mean translocation time $\langle \tau \rangle$ for the case where no bias force F is applied, as a function of chain length N . The inset shows the corresponding plots for the gyration radii where the diamonds, circles, squares, represent the gyration radii, and the longitudinal and the transverse components R_{gl} and R_{gt} respectively.

Fig. 2: (a) Mean first passage time (MFPT) for forced translocating chains. Different colors correspond to $N=16$ (black), $N=32$ (red), $N=64$ (green), $N=128$ (blue) and $N=256$ (orange). (b) MFPT normalized by the $\langle \tau(N) \rangle$ as a function of normalized chain segment m/N for $N=16$ (top curve) to $N=256$ (bottom curve). The dashed straight line (magenta) corresponds to the line of unit slope for comparison

Fig. 3: Location of the $Z_{CM}(N/2)$ for several different chain lengths plotted vs. the index labelling the individual simulation runs. The dots represent data points from each run. The dashed red line correspond to the $\langle Z_{CM}(N/2) \rangle$ averaged over all these points. The position of $Z = 0$ is denoted by the solid black line for easy comparison.

Fig. 4: Plot of $Z_{CM}(N/2)$ as a function of chain length for several different bias values. The circles, squares, diamonds, and triangles correspond to the bias values $F=12.0$, $F=6.0$, $F=4.0$, and $F=2.0$ respectively.

Fig. 5: (a) Plot of $\langle Z_{CM}^{cis}(m) \rangle$ (dashed black, red and green) and $\langle Z_{CM}^{trans}(m) \rangle$ (solid blue, orange, and magenta) as a function of the segments on the *cis* and *trans* side for chain lengths $N = 65, 129$ and 257 respectively for unbiased translocation. (b) the corresponding plot on the log-log scale where we notice that for a large fraction of the *cis* and *trans* segments $\langle Z_{CM}(m) \rangle \sim m^{0.57}$.

Fig. 6: (a) Plot of $\langle Z_{CM}^{cis}(m) \rangle$ (black, red and green) and $\langle Z_{CM}^{trans}(m) \rangle$ (blue, orange, and magenta) as a function of the segments on the *cis* and *trans* side for chain lengths $N=64, 128, \text{ and } 256$ respectively for forced translocation. Note that the data for $\langle Z_{cm}^{trans}(m) \rangle$ for different N coincide almost perfectly on a common curve, so one can hardly distinguish the individual values for $m < 64$ on this plot; (b) the corresponding plots on log-log scale. Straight lines indicate the power laws quoted in the figure.

Fig. 7: Plot of gyration radii $\langle R_g(t) \rangle$ as a function of time for the unbiased (top) translocation and (bottom) for the forced translocation where a significant variation of the size of the

translocating chain is immediately noticeable. In each figure that double-dotted (black and blue) lines represent the longitudinal components, wide dashed (red and orange) lines represent the transverse components and the solid lines (green and magenta) correspond to the gyration radii for chain lengths 65(64) and 129(128) for the unbiased(biased) translocation respectively. The thin straight lines in each case (with the same symbols) correspond to the corresponding time averaged values. Note that $\langle R_g(t) \rangle > \langle R_{gt}(t) \rangle > \langle R_{gl}(t) \rangle$ for unbiased translocation.

Fig. 8: Plot of (log-scale) (a) $\langle R_{gt}^{cis}(m) \rangle$, $\langle R_{gt}^{trans}(m) \rangle$, (b) $\langle R_{gl}^{cis}(m) \rangle$, $\langle R_{gl}^{trans}(m) \rangle$, and (c) $\langle R_g^{cis}(m) \rangle$, $\langle R_g^{trans}(m) \rangle$ as a function of the segments m on the *cis* and *trans* sides respectively, for the case of unbiased translocation. The straight line (purple) in each figure refers to the slope. The inset of (b) compares the longitudinal component (upper curve) $\langle R_{gl}(m) \rangle$ and the transverse component (lower curve) $\langle R_{gt}(m) \rangle$ for chain length $N=129$ for comparison.

Fig. 9: Plot of (log-scale) (a) $\langle R_{gt}^{cis}(m) \rangle$, $\langle R_{gt}^{trans}(m) \rangle$, (b) $\langle R_{gl}^{cis}(m) \rangle$, $\langle R_{gl}^{trans}(m) \rangle$, and (c) $\langle R_g^{cis}(m) \rangle$, $\langle R_g^{trans}(m) \rangle$ as a function of the segments m on the *cis* and *trans* sides respectively. In each figure the solid and dotted lines correspond to the *cis* and *trans* components respectively. Note that the curves for the *trans* part (lower set of dashed curves in each part of the figure) superimpose to such a large extent that they are hardly distinguishable from the data for $N = 256$ in these figures.

Fig. 10: Plot of the radius of gyration $\langle R_g \rangle$ and end to end distance $\langle R_{1N} \rangle$ (logarithmic scale) of the chain which has just translocated as a function of the chain length N (logarithmic scale). The solid(open) circles (black) and squares (red) refer to the forced(unbiased) translocation.

Fig. 11: (a) Plot of longitudinal (solid lines) and transverse (dotted lines) components of gyration radii for the polymer which has just translocated as a function of the monomer index m for unbiased translocation. The solid black, red, and green lines correspond to the longitudinal components and dotted blue, orange, and magenta lines correspond to the transverse components for chain lengths $N=65$ and $N=129$ respectively. (b) the plot on a log-log scale.

Fig. 12: Plot of gyration radii for the chain segments of length $n = 16$ for chain length $N = 256$ at different stages of the translocation process when integral number of chain

segments n_i have translocated. The vertical red lines differentiate the *trans* and the *cis* segments. The filled squares and diamonds represent the longitudinal and the transverse components of the gyration radii respectively and the filled circles represent the the gyration radii.

Fig. 13: Plot of gyration radii for the chain segments of length $n = 32$ for chain length $N = 256$ at different stages of the translocation process when integral number of chain segments n_i have translocated. The vertical red lines differentiate the *trans* and the *cis* segments. The filled squares and diamonds represent the longitudinal and the transverse components of the gyration radii respectively and the filled circles represent the the gyration radii.

Fig. 14: (a) Plot of longitudinal (solid lines) and transverse (dotted lines) gyration radii for the polymer which has just translocated as a function of the monomer index m . The solid black, red, and green lines and dotted blue, orange, and magenta lines correspond to the chain lengths $N=64, 128,$ and 256 for the longitudinal and transverse components respectively. (b) the same plot on a log-log scale.

Fig. 15: The distribution of longitudinal (circles) and transverse (squares) components of the end to end distances of a chain which has just translocated for chain lengths $N=128$ (top) and $N=256$ (bottom). For comparison the corresponding equilibrium configurations for the longitudinal (diamonds) and transverse (triangles) components at the *cis* side at the beginning of each translocation run are also shown.

Fig. 16: Contemplated defect schematic in the vicinity of the pore. The range of segment number m over which a change of the effective exponent is observed increases with increasing size of the subchain that is considered.

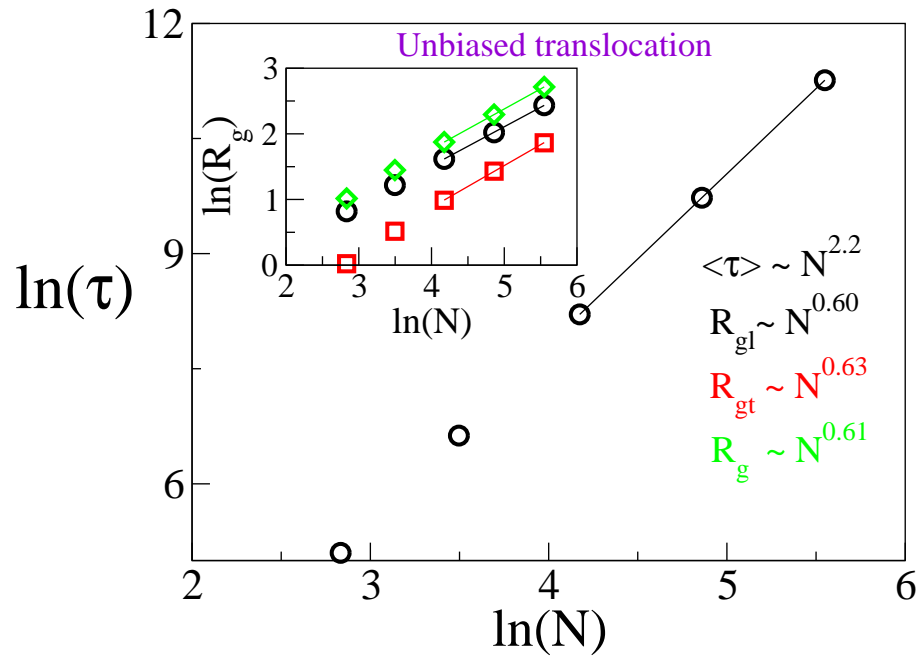


FIG. 1:

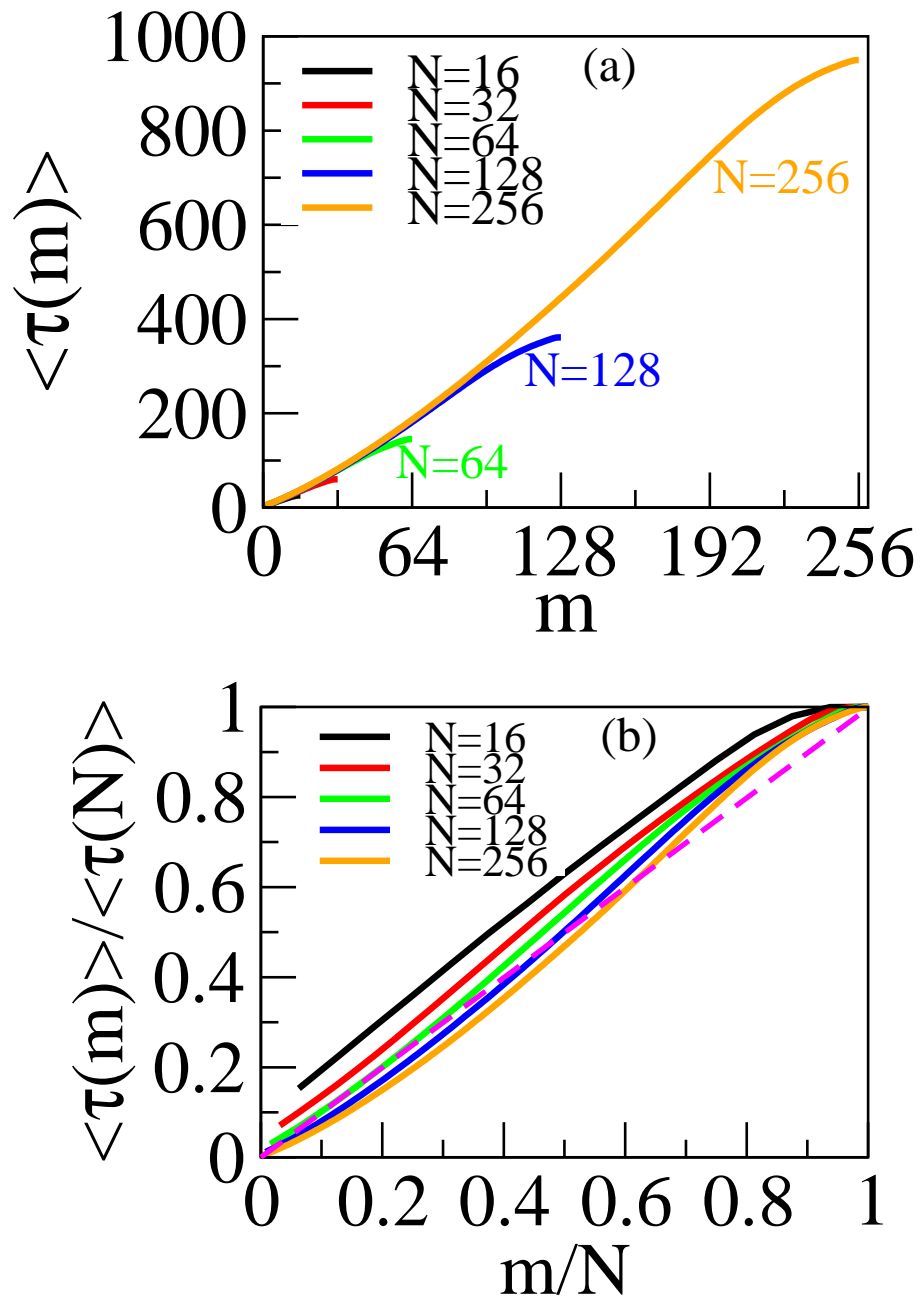


FIG. 2:

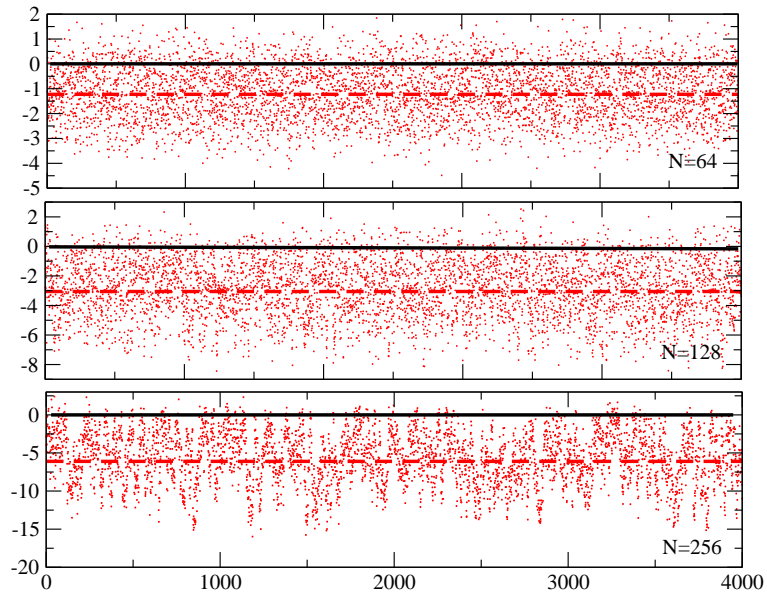


FIG. 3:

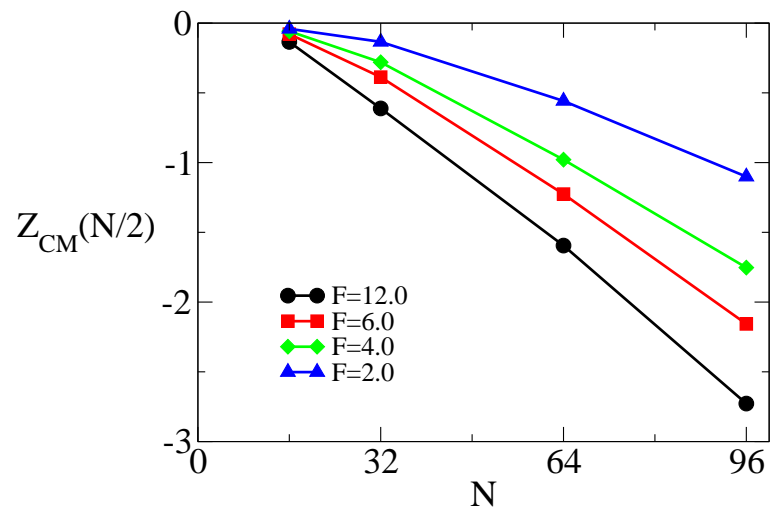


FIG. 4:

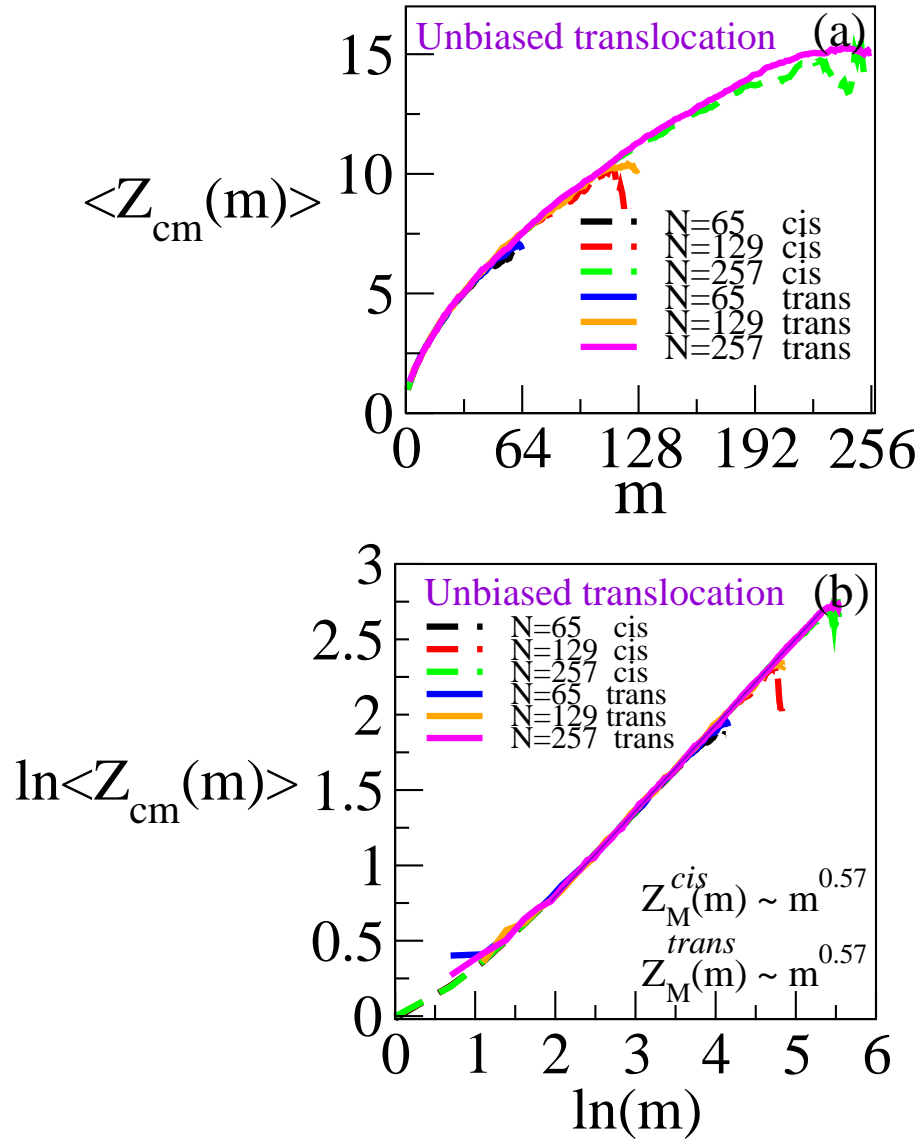


FIG. 5:

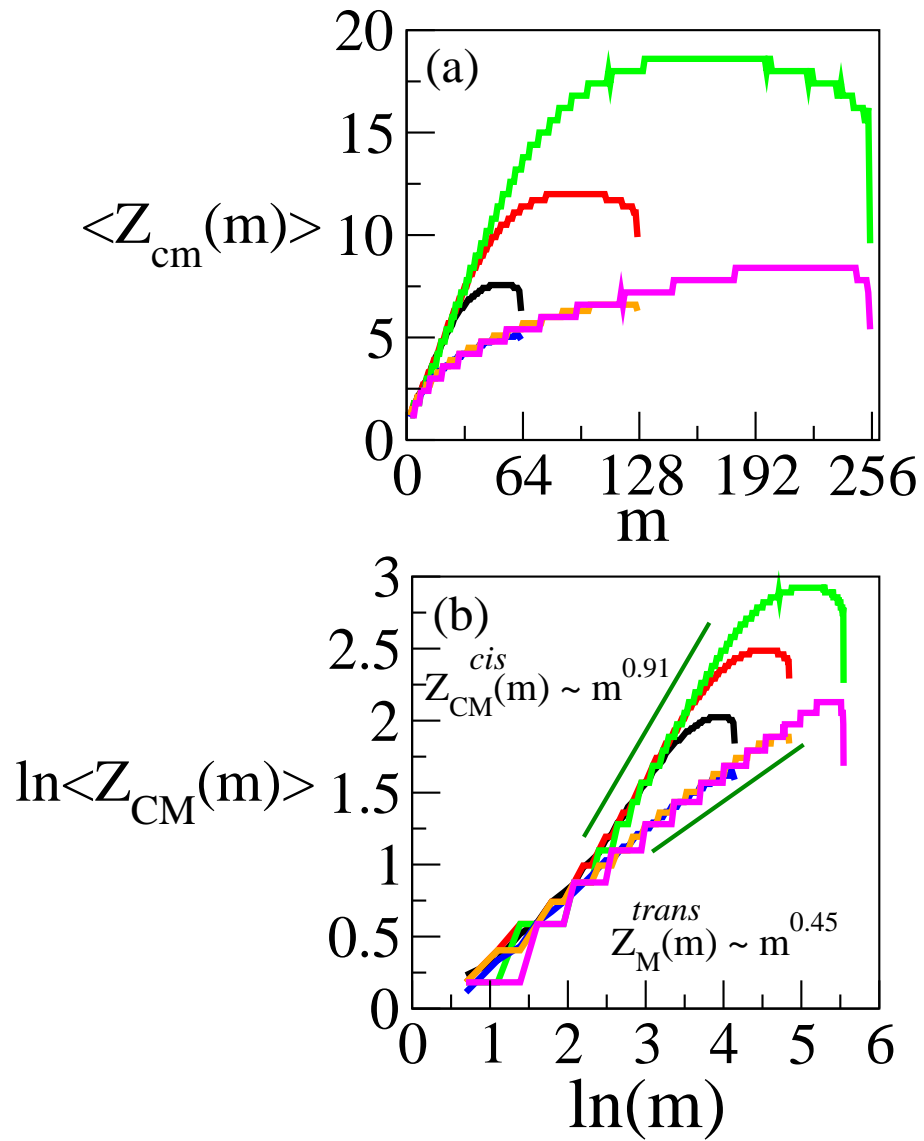


FIG. 6:

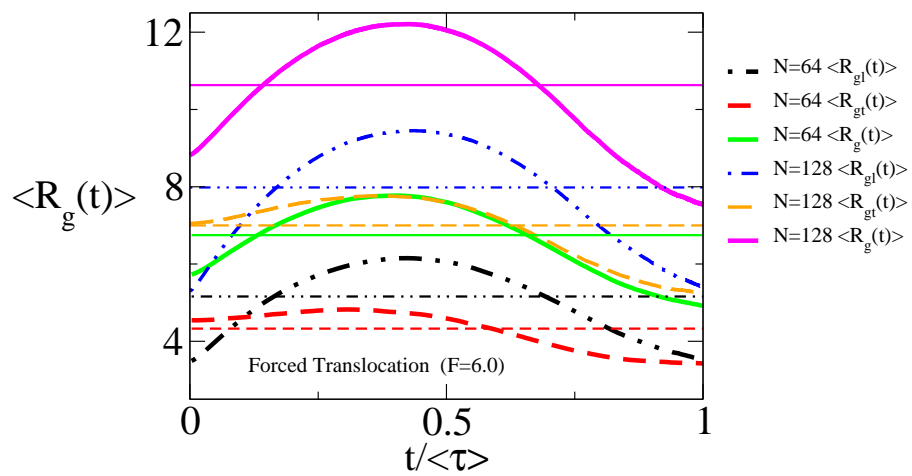
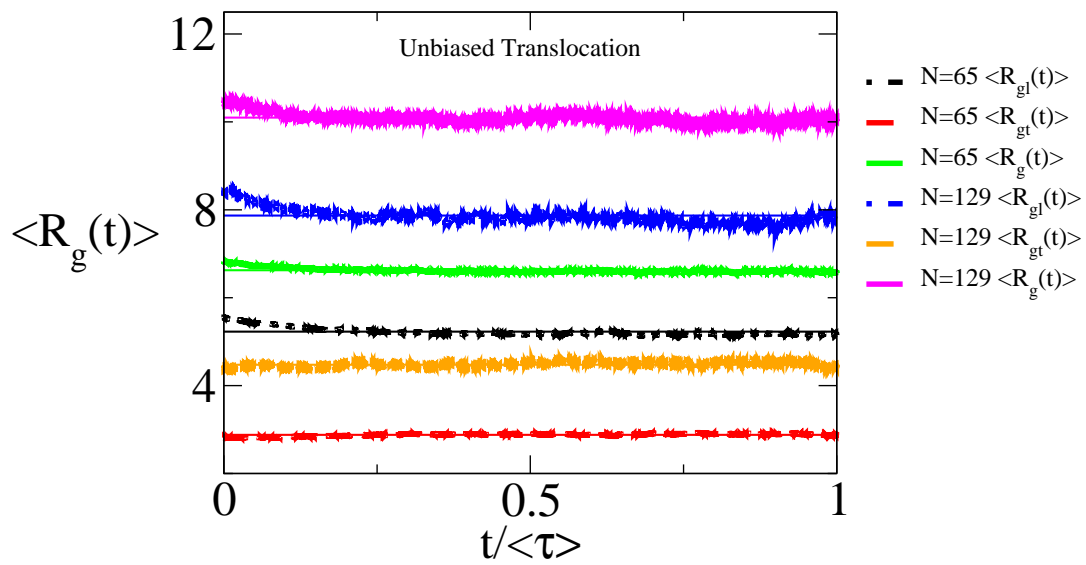


FIG. 7:

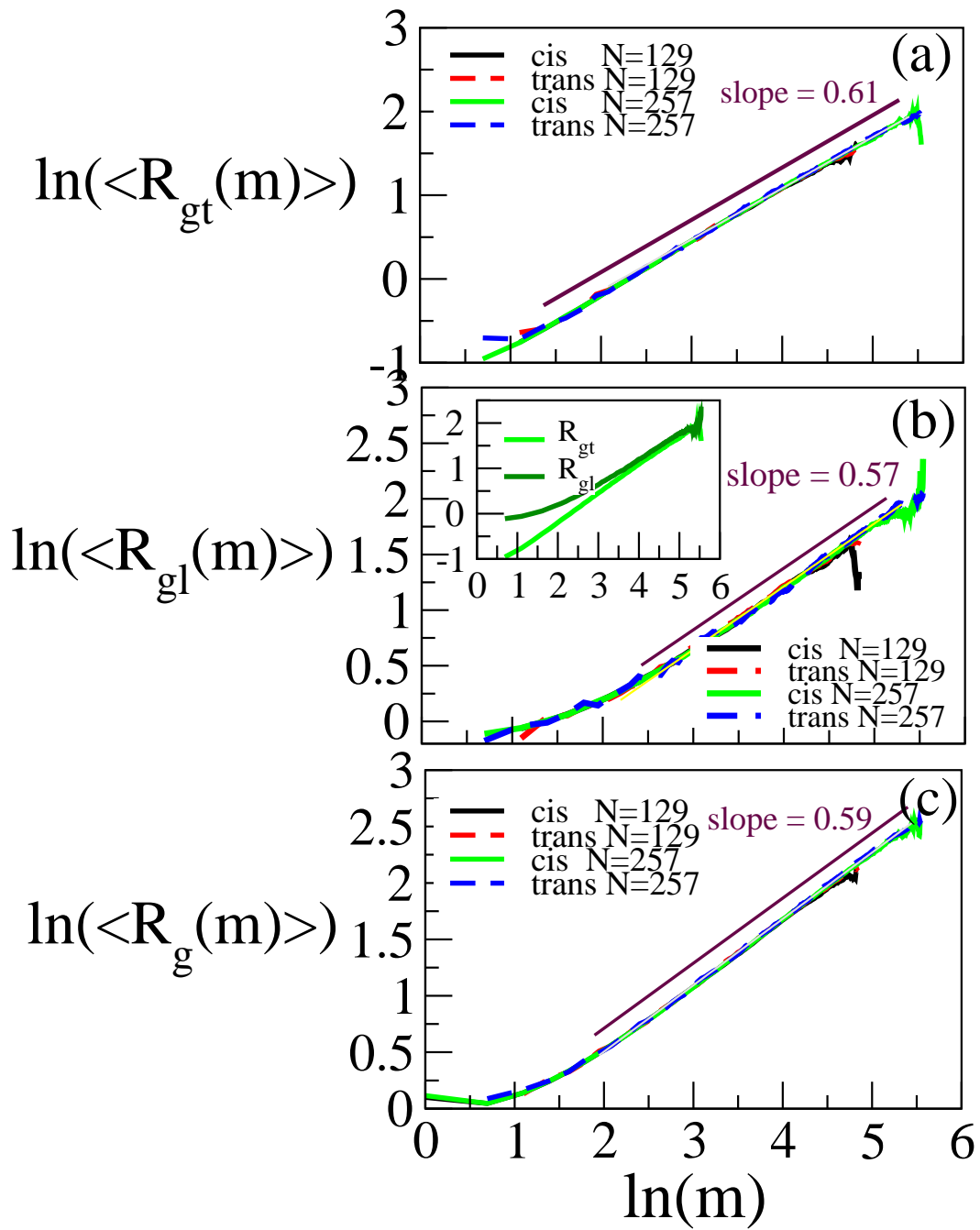


FIG. 8:

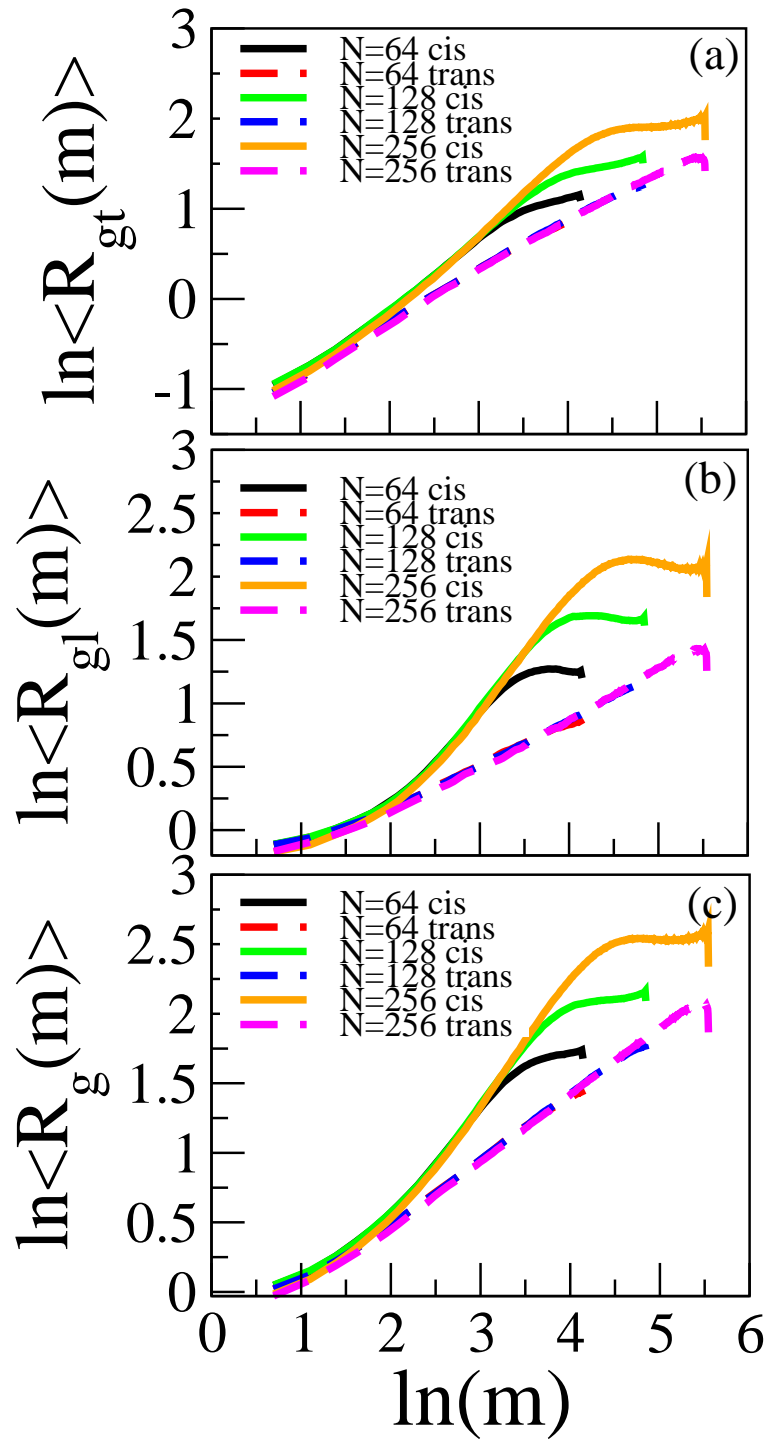


FIG. 9:

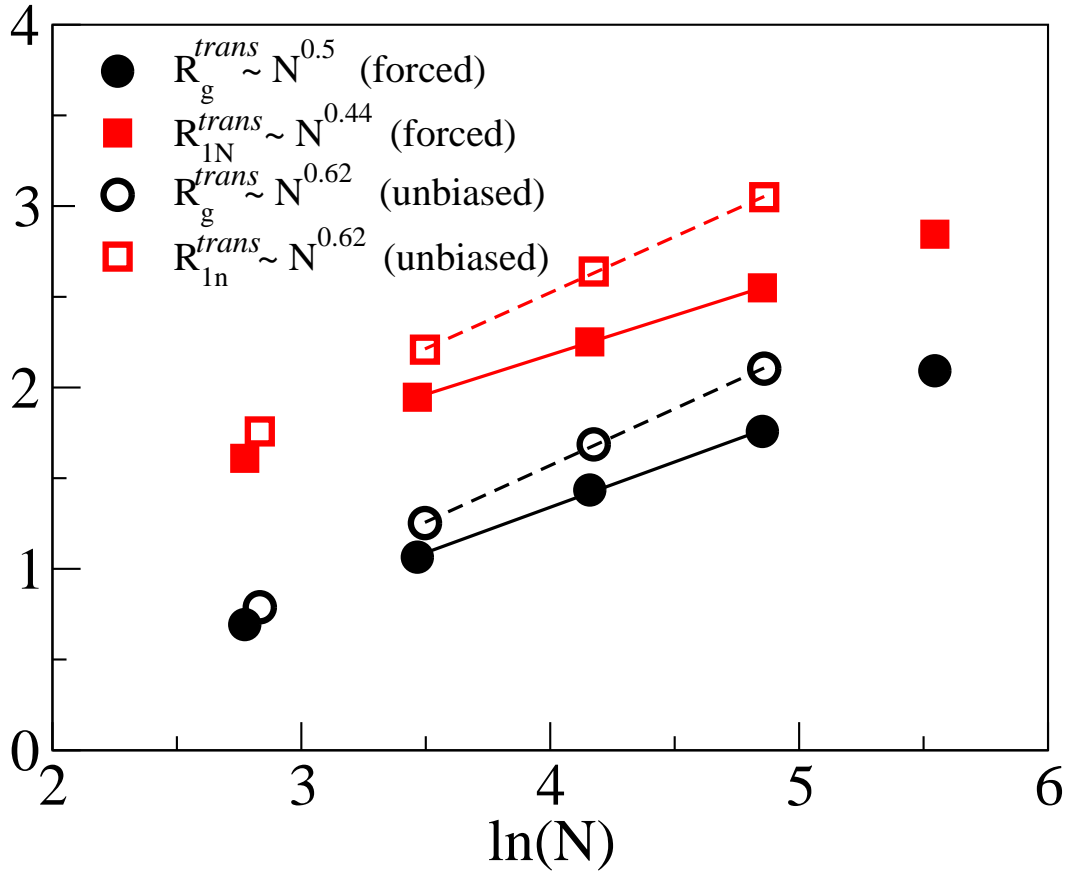


FIG. 10:

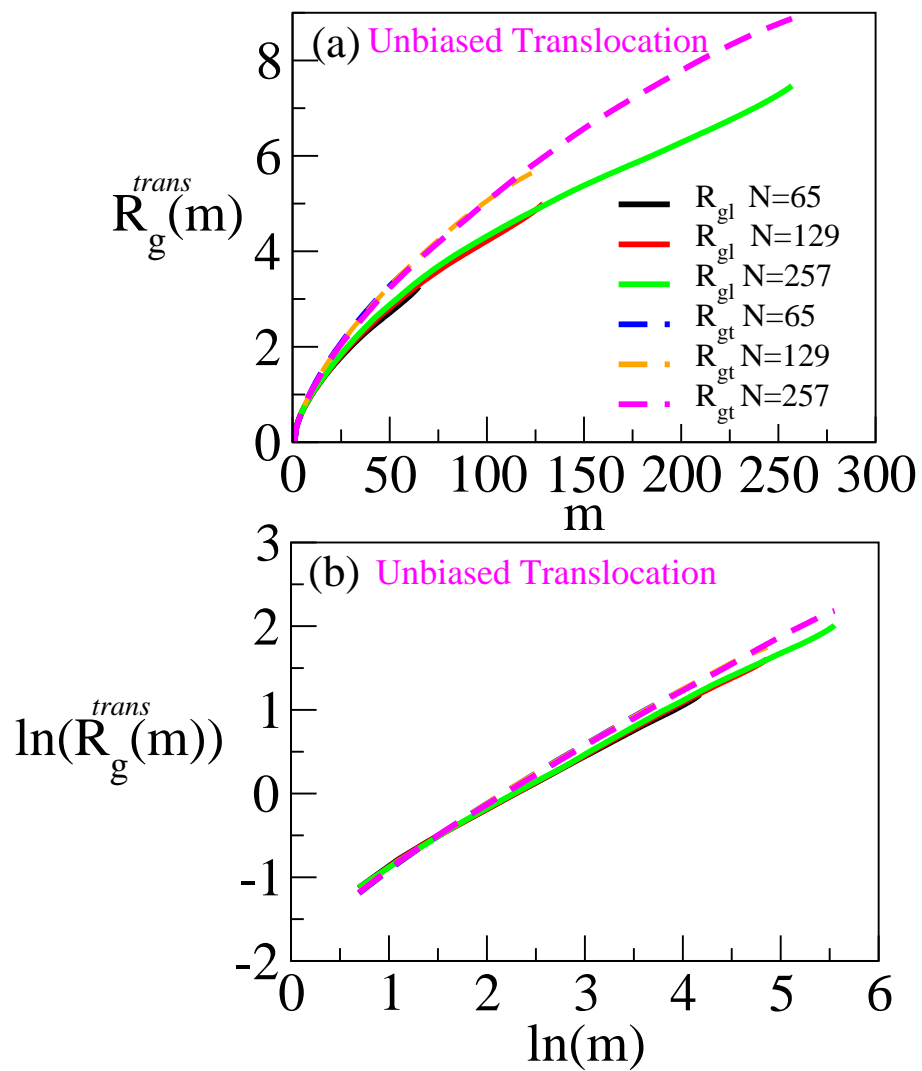


FIG. 11:

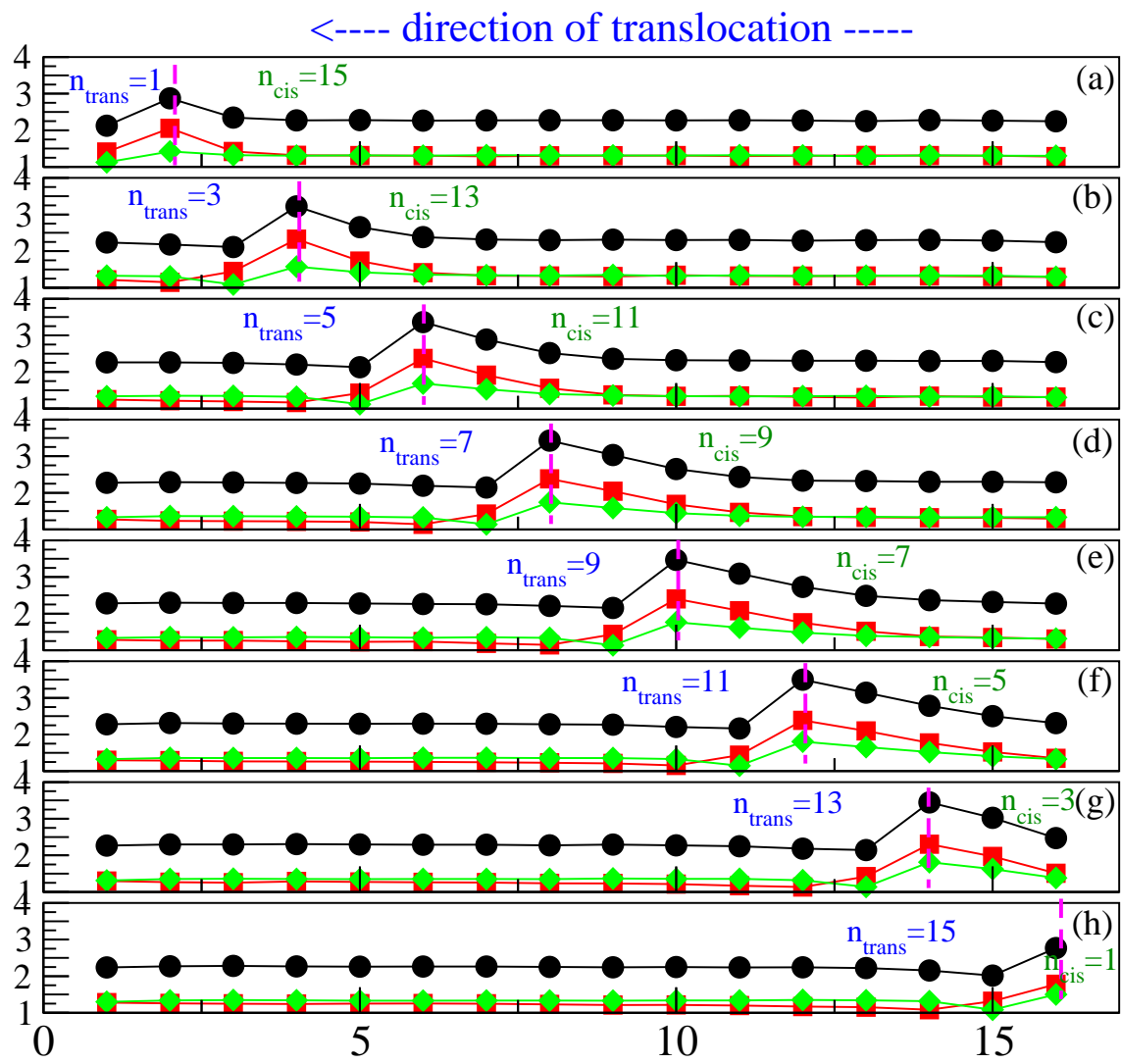


FIG. 12:

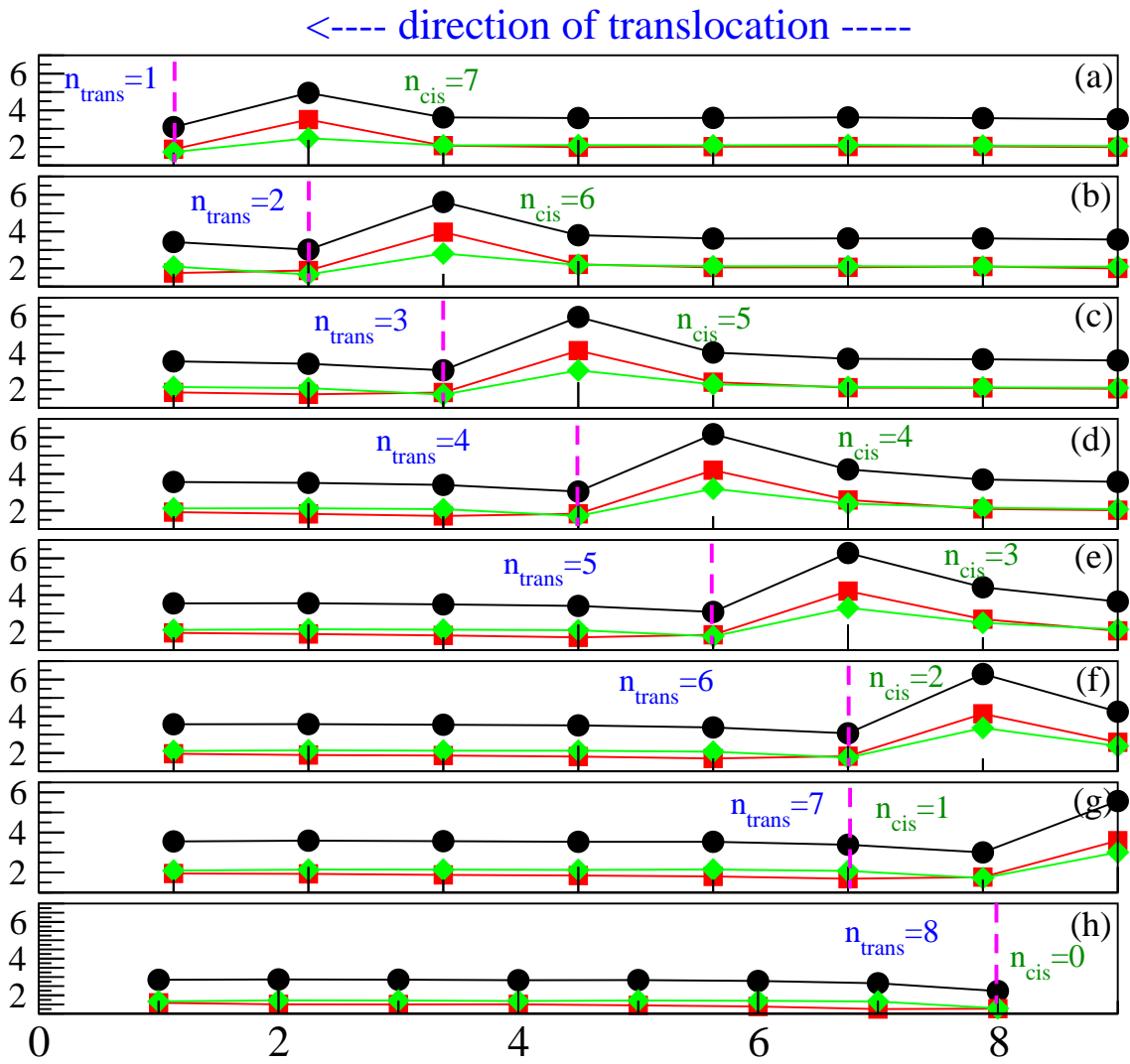


FIG. 13:

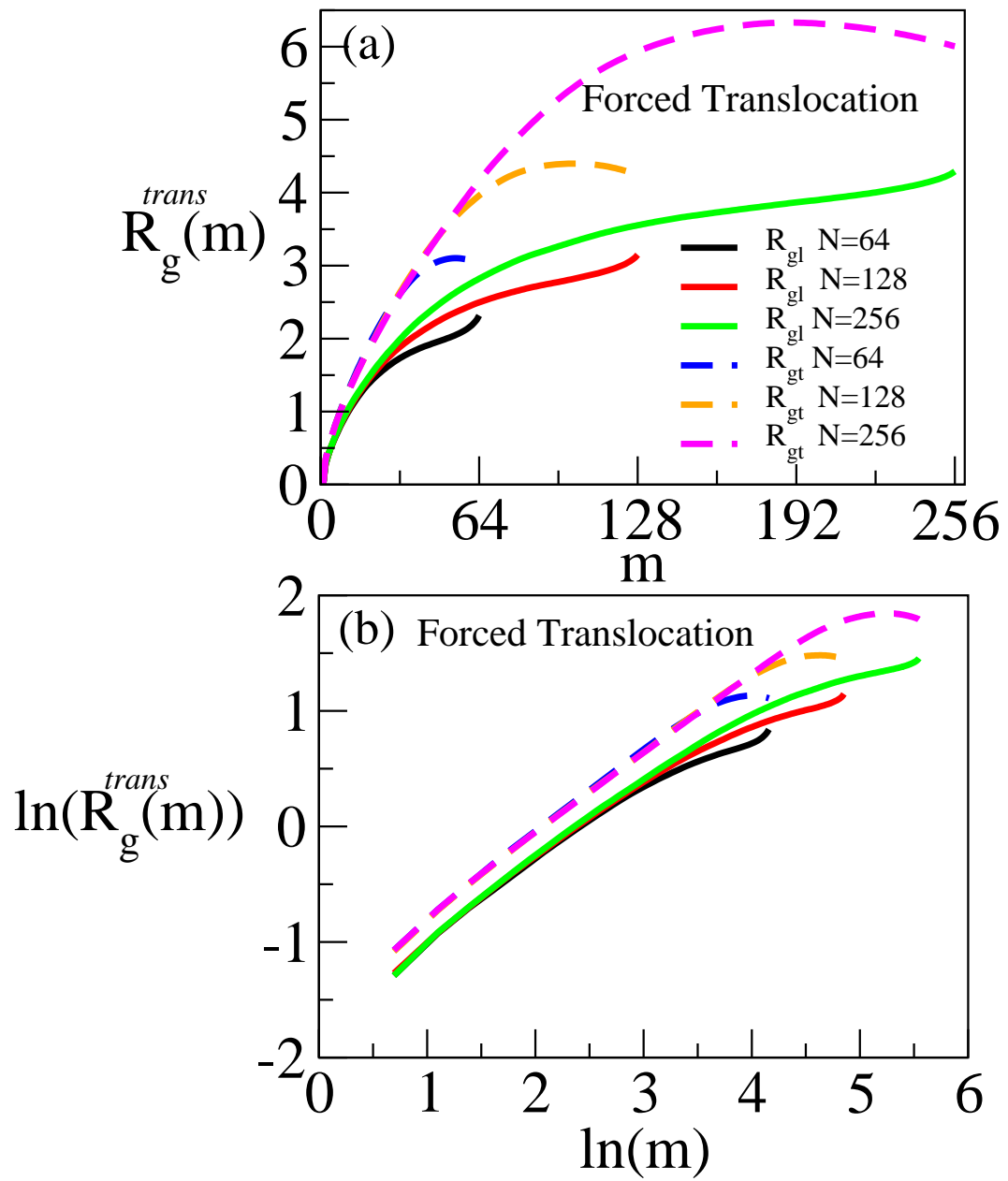


FIG. 14:

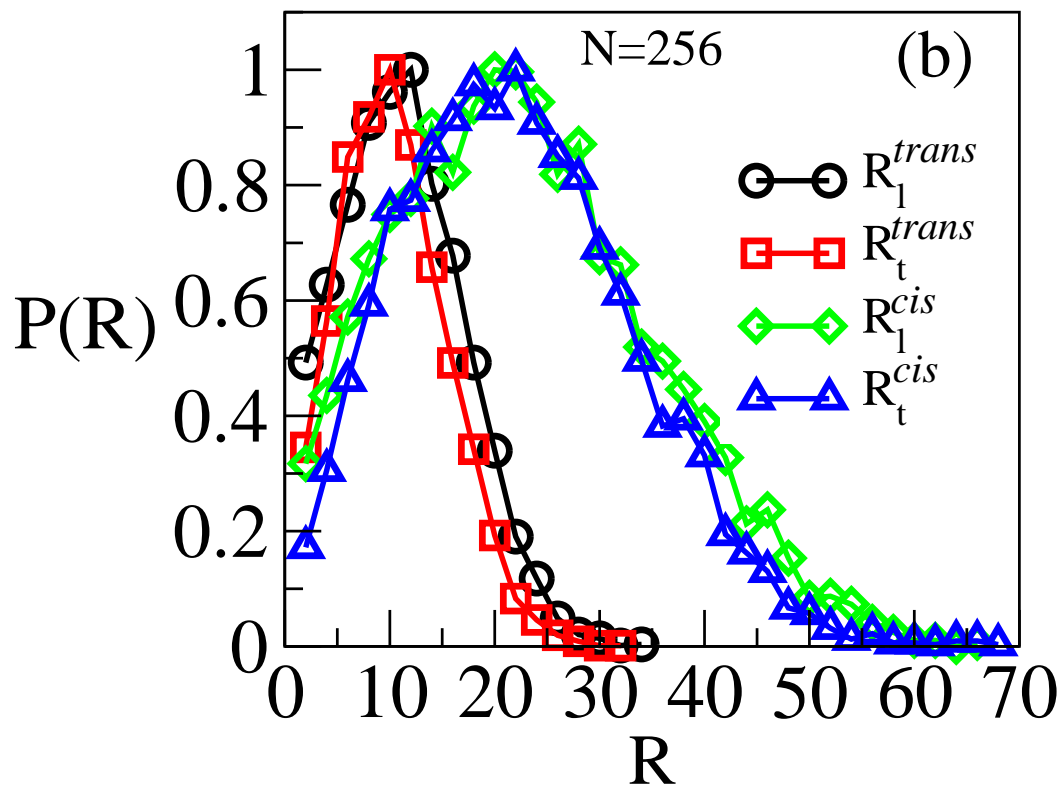
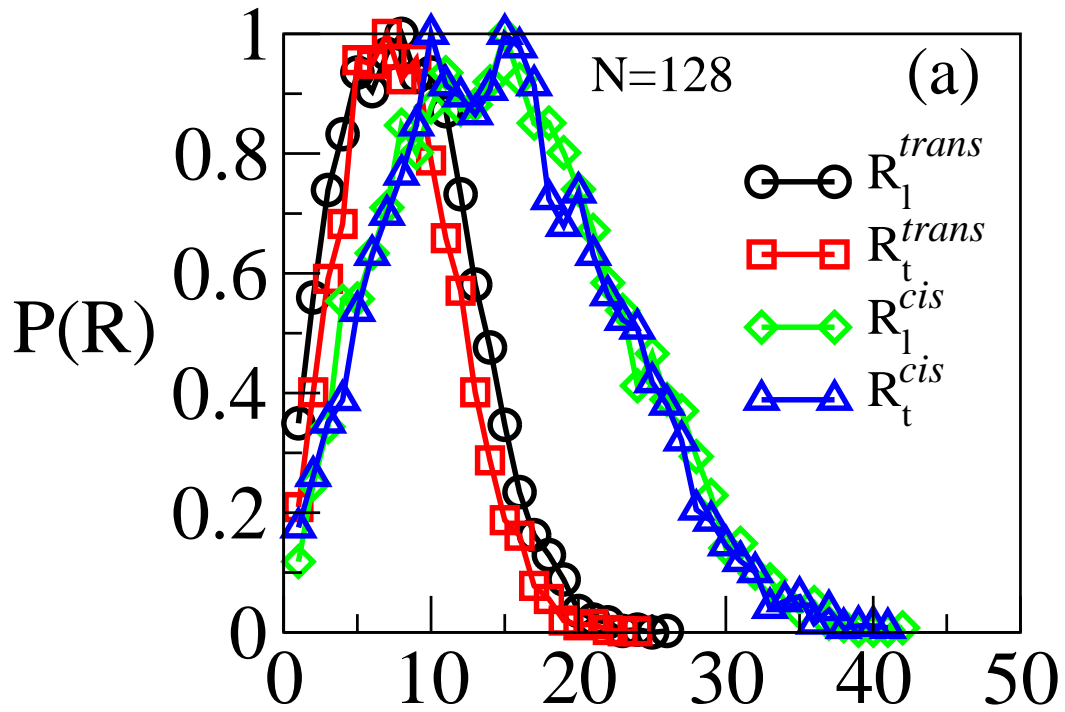


FIG. 15:

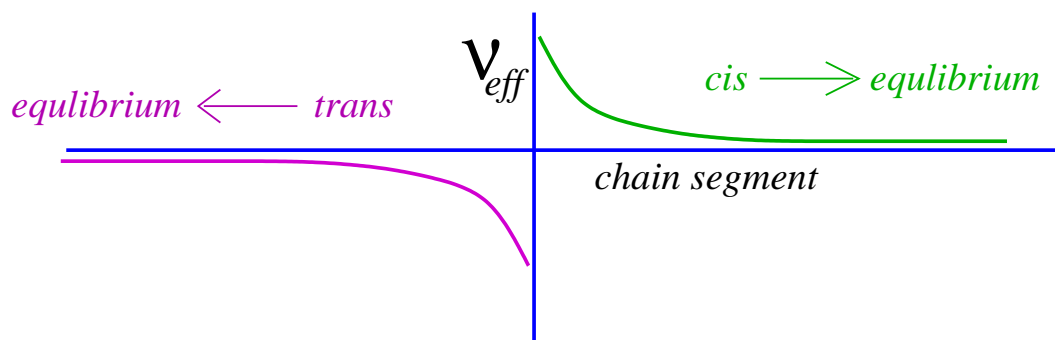


FIG. 16: